Physical origin of wave breaking: from longitudinal dust acoustic waves to transverse water surface waves

Ue-Yu Pen, Mei-Chu Chang, and Lin I

Department of Physics and Center for Complex Systems, National Central University, Jhongli, Taiwan 32001, Republic of China

Wave breaking followed by the sudden drop of the wave amplitude after wave steepening is a ubiquitous nonlinear phenomenon. It occurs in transverse and longitudinal waves, such as water surface waves [1, 2], electron density waves in plasmas [3], dust acoustic waves in dusty plasmas [4], etc.. Eulerian approach has been mainly used in the past studies. In this work, by direct tracking the individual particle motion in dust acoustic waves self-excited in dusty plasma and in water surface waves approaching a slope, the Lagrangian-Eulerian pictures for wave breakings of both waves are constructed and compared.

Breaking of the Self-excited Dust Acoustic Wave

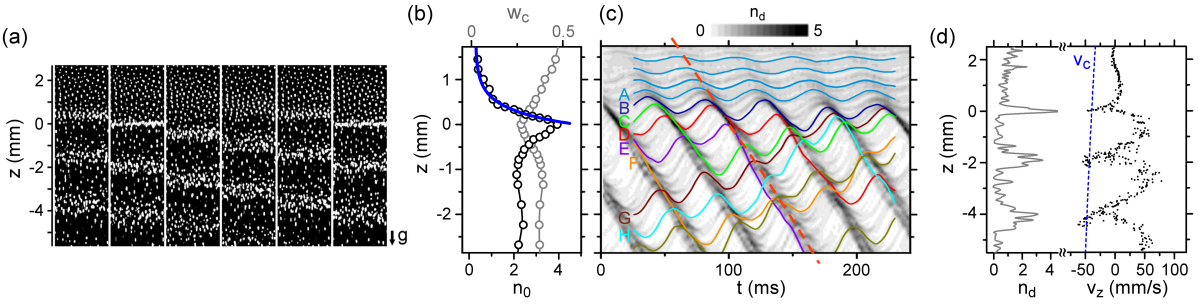

Figure 1: (a) The sequential snapshots of the dust images with 1 ms exposure time and 10 ms interval. (b) The average spatial variations of the normalized wave amplitude n_0 and the wave width w_c. (c) The temporal dust vertical trajectories on top of the evolution of the normalized dust density $n_d(z,t)$. (d) The $z-v_z$ phase-space distribution of dusts at the phase $\phi = 0$ of the wave oscillating cycle, where $\phi = 0$ is defined as one of the crests reaches $z = 0$ mm. Each dot represents the state of one dust. The tilted dashed line is the spatial variation of crest velocity v_c. The gray line depicts the corresponding spatial dust density waveform distribution [4].

The experiment is conducted in a cylindrical symmetric rf discharge dusty plasma system, in which the weakly ionized glow discharge is generated in 200 mTorr Ar using a 14-MHz rf power system as described elsewhere [4]. Polystyrene dust particles (5 μm in diameter) are confined and suspended in plasmas. In the presence of the downward ion flow providing a free energy source, the downward propagating dust acoustic wave (DAW) with longitudinal dust

oscillations can be self-excited by increasing rf power to 2.6 W. The dust images illuminated by a thin vertical laser sheet are recorded by a CCD at 500 Hz frame rate.

Figure 1(a) shows the typical sequential snapshots of dust images, where the bright dense regions are the wave crest regions and $z = 0$ mm indicates the position of wave breaking. The normalized dust density $n_d(z,t) = I_d(z,t)/\langle I_d(z)\rangle$ is measured, where $\langle I_d(z)\rangle$ is the time average of the scattered laser light intensity $I_d(z)$, coarse grained over the rectangle 0.1 mm in height and 2.5 mm in width at height z. Figure 1(b) depicts the average spatial variations of the normalized wave amplitude n_0 and the wave width w_c [measured at $n_d = 1$ and normalized by the wave period $\tau = 1/f_0$ (the wave frequency $f_0 = 22.5$ Hz)]. It is found that the DAW has a small wave amplitude n_0 in the upper region. The waveform steepens associated with the growth of wave amplitude n_0 and the decrease of wave width w_c along the descending z. The DAW breaking occurs at $z = 0$ mm, where the wave crest has the narrowest width and the maximum height. After breaking ($z < 0$ mm), the wave amplitude and the crest width reach another constant level. Figure 1(c) shows the temporal dust vertical trajectories on top of the evolution of the normalized dust density $n_d(z,t)$. Before breaking, dusts exhibit small amplitude coherent oscillations [see the dust motions above dust A in Fig. 1(c)]. Around breaking ($z = 0$ mm), the onset of chaotic dust motion is associated with the onset of trajectory crossing of nearby dust pairs. After breaking, dusts exhibit chaotic motion. Some dusts still can reach the crest rear but some dusts are trapped in the crest front with uncertain trapping time [see the long downward trajectories of dust C to F in Fig. 1(c)]. Figure 1(d) depicts the $z - v_z$ phase-space distribution of dusts associated with the spatial dust density waveform distribution and the z dependent crest velocity.

Breaking of the Shallow Water Surface Wave

The experiment is conducted in an acrylic water tank [8 cm in inner width and 4 m in length, with a sloped floor (7^o inclination) 2 m in length at the end], as described elsewhere [2]. The still water surface ($z = 0$ cm) is 17 cm above the horizontal bottom floor before the inclined floor. The water wave approaching the slope is periodically generated by a motor-driven paddle at 1.43 Hz. The tracers with 0.99 g/cm^3 mass density are digitally recorded by a CCD with 300 Hz sampling rate.

Figure 2(a) depicts the sequential waveforms at 1/30 s time interval. After the gradual steepening of the wave front with the increasing x, wave breaking onsets at $t = 0$ s and $x = 0$ cm associated with the formation and the subsequent curling of the overhanging plunger which eventually touches the water surface ahead. Figure 2(b) to (d) show the tracer trajectories in the $x - z - t$ space with the waveform evolution, in the $x - t$ space with the contour plot of the water

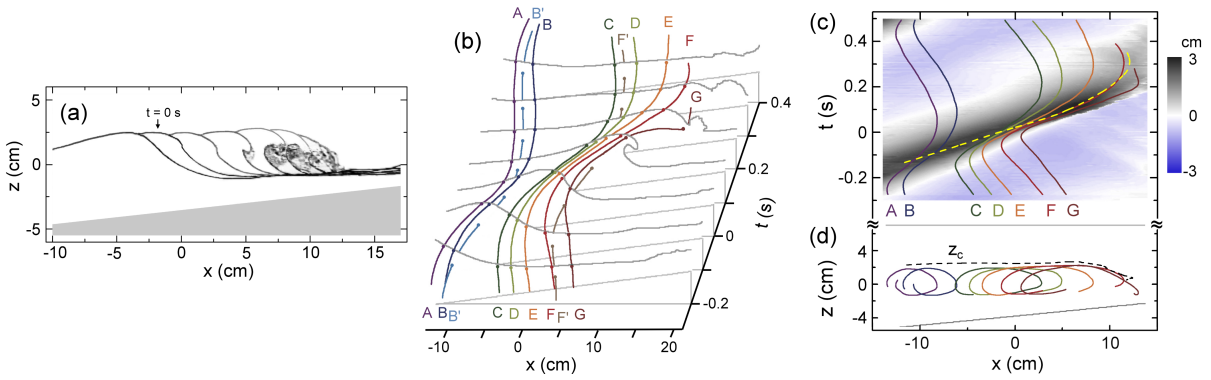

Figure 2: (a) The sequential waveforms at 1/30 s time interval. (b) The evolution of tracer trajectories in the $z-x-t$ space. The dots on tracer trajectories show their $z-x$ positions at the times for taking the snapshots of the waveforms indicated by the gray solid curves. The tilted straight light gray lines correspond to the inclined floor. (c) The tracer trajectories on the contour plot of the water surface height z in the $x-t$ space. The dashed line is the trajectory of the wave crest. (d) The tracer trajectories in the $x-z$ space. The dashed line and the tilted straight gray line show the x dependences of the crest height z_c and the floor heights z_f, respectively [2].

surface height z, and in the $x-z$ space with the x dependence of the crest height z_c, respectively. It is observed that, before breaking ($x < 0$ cm), the surface tracers (e.g. tracers A to D) exhibit coherent cyclic motion in the $x-z$ space with small forward Stokes drift and slow divergence of the trajectories of adjacent tracers. The leftward moving surface tracers [e.g., tracers A to D in Fig. 2(a) and (b)] entering the crest front are pushed rightward and upward by the crest front. They then move rightward more slowly than the crest while reaching the crest top, and are finally reaccelerated leftward as they slide down the crest rear. At breaking, the surface tracers F and G are unable to climb over the steepened crest front. They curl up, move forward and form the plunging jet. However, the lower tracers [e.g. tracer F'] still can reach the crest rear. The onset of wave breaking leads to the transition to the chaotic oscillation with the rapid divergence of the adjacent surface tracer trajectories [see the trajectories of tracers D, E and F].

Common Origins of the Breakings of the Above Two Waves

The breakings of the dust acoustic wave and the shallow water wave share the common feature of the sudden wave amplitude drop as the crest front steepening reaches a certain critical value. Now let us construct the Lagrangian-Eulerian picture to explain how the dust (fluid element) motion constitutes the waveform evolution which in turn affects the dust (fluid element) motion. In the wave frame of the dust acoustic wave (the water surface wave), the kinetic energy of the charged dust (the fluid element) can be exchanged with the electrostatic potential

energy (the gravitational energy) as the dust (fluid element) climbs up and slides down the wave crest. The acceleration and deceleration of dusts (fluid elements) entering the crest front and the crest rear cause their compression (accumulation) and rarefaction (depletion) in the above two regions, respectively. It leads to the steepening and the advancing of the propagating wave in the laboratory frame. The wave crest front steepening instability eventually prevents the surface fluid and part of the incoming dusts from climbing over the crest top to the crest rear. The associated suppression of feeding dusts (fluid elements) to the crest top leads to wave breaking with the drop of the crest height.

The two dimensional motion in the transverse water wave makes its wave breaking more complicated than that of the one dimensional longitudinal density wave. The extra degrees of freedom for the water wave allow the surface layer moving leftward to the steepened wave crest to reverse its direction after curling up, and to form a plunging jet leading the breaking wave front. Comparing with the incompressible water surface wave, the longitudinal density variation provides the extra dimension. Only part of the dusts entering the crest front is able to climb over the crest and move into the crest rear. The dusts with insufficient kinetic energy are trapped in the crest front, and form an overhanging plunger in the $z - v_z$ phase space. Namely, similarly to the water wave breaking, right ahead of the crest, the dusts and the fluid elements have the double value distributions. In both waves, the onset of wave breaking leads to the transition from the coherent particle oscillation to the chaotic particle oscillation with rapid divergence of the trajectories of the adjacent particle pair.

Acknowledgment

This work is supported by the National Science Council of the Republic of China under contract No. NSC99-2112-M008-002-MY3.

References

[1] D. H. Peregrine, Annu. Rev. Fluid Mech. **15**, 149 (1983). M. L. Banner and B. H. Peregrine, Annu. Rev. Fluid Mech. **25**, 373 (1993).

[2] U. Y. Pen, M. C. Chang, and L. I, submitted to Phys. Rev. E.

[3] J. A. Dawson, Phys. Rev. **113**, 383 (1959). M. N. Rosenbluth and C. S. Liu, Phys. Rev. Lett. **29**, 701 (1972).

[4] L. W. Teng, M. C. Chang, Y. P. Tseng, and L. I, Phys. Rev. Lett. **103**, 245005 (2009).